

# Compact FPGA based Multi-Axial Interferometer Applied in a Metrological Atomic Force Microscope

**Sebastian Strube, Gabor Molnar, Hans-Ulrich Danzebrink,**  
Physikalisch-Technische Bundesanstalt (PTB), Braunschweig

## Abstract

For use in a new, metrological atomic force microscope (AFM) a highly compact interferometer, based on a modified homodyne Twyman-Green interferometer concept was developed at PTB. It is modular, measures displacement and tilt simultaneously, allows for traceability and an uncertainty in the Ångstrom range. A novel signal processing approach based on a field programmable gate array (FPGA) is employed, whereby a spatial interferogram is acquired by a high-speed line sensor and transformed into its frequency spectrum through a discrete Fourier transform. The AFM combines an FPGA for preprocessing, a digital signal processor (DSP) which runs the AFM control algorithm and a general purpose processor (GPP) for user-interface handling and mass data storage. The complete system allows for implementing a multitude of different AFM measuring modes, e.g. contact mode, intermittent contact mode using amplitude detection and phase detection or frequency tracking mode.

**Keywords:** interferometry, FPGA, nanometrology, nanoscale, atomic force microscopy (AFM), nanopositioning, tilt measurement, distance measurement

## 1. Introduction

Sensors implemented in AFM closed-loop positioning stages are usually based on capacitive [1, 2], inductive [3], or interferometric methods [4-7]. Capacitive sensors suffer from noise, especially if used with small diameters in highly compact positioning stages, and from nonlinearity that needs to be compensated for. Furthermore, direct traceability using capacitive and inductive sensors is not possible. Apart from the determination of the stage position, also the measurement of its tilting due to guidance errors, resulting in Abbe errors, is another task to be fulfilled in precision scanning systems.

For use in PTB's new AFM an interferometric sensor design was developed that is compact, traceable, and measures displacement and tilt simultaneously with a sub-Ångstrom uncertainty. Other applications for this sensor concept could also involve longer ranges with

lower uncertainties (limited only by the coherence length of the light source used), for instance as a substitute for length measurement systems in drilling or milling machines.

## 2. AFM system overview

The design of a completely open AFM system is anticipated by our working group to give full control over and insight into hardware and software used for positioning, data acquisition, filtering and feedback control.

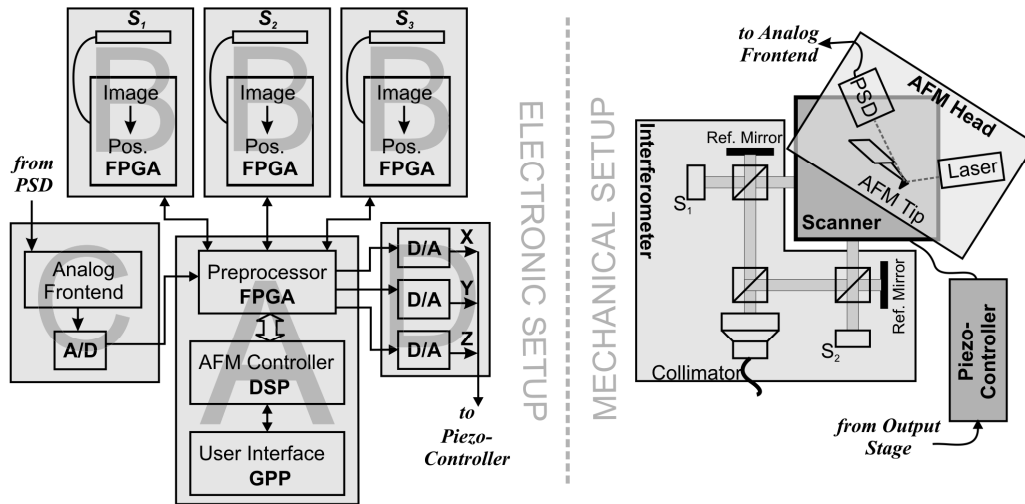


Fig. 1: Electronic setup (modules A,B,C,D, left). Mechanical setup (right).

The system blocks are encapsulated in modules which permit an easy exchange of individual components. Additionally a reuse of modules in/from other projects is feasible and intended. The **main module** of the current system is shown in figure 1.A. It consists of a floating-point DSP core combined with a general purpose processor (GPP) [8] combined in a single package, connected over fast communication busses, which eases debugging and data collection. The GPP runs a standard Linux system (Kernel 2.6.33, patched for our add-on hardware) which supports LAN, USB 2.0 (as host and device) and SATA for data storage and control. SSH and HTTP are used to access the main module over network. The DSP currently runs stand-alone code, but for more complex tasks a realtime operating-system (e.g. SYS/BIOS) can be used. Its program code is loaded through the GPP. An FPGA (Spartan 3A, XC3S400A) is connected over a 16Bit wide external memory interface and mapped into the address space of both DSP and CPU.

The **interferometric position sensor modules** are shown in figure 1.B. They are based on a high resolution black/white image sensor (EV76C560 [9], 1280x1024 pixel) and an image processing FPGA (Xilinx Spartan 3A XC3S200AN or XC3S3400ADSP). In the current setup the image sensor operates in single line mode, to achieve the highest possible frame rate,

however a multitude of configurations is possible. Different communication add-on cards can be connected to the positioning module to add needed interfaces (e.g. serial peripheral interface (SPI), fibre Interface, USB, VGA, HDMI), which gives the modules high versatility.

The **tip data acquisition module** is shown in figure 1.C. In the current setup two A/D converters (AD7667, 16Bit, 1Msps) are used for input digitization of the tip signal (preprocessed in the analogue domain). The tip acquisition front-end can consist of an AM or FM detector or can be exchanged to contain any other detection variant. Tip excitation and quadrature signal generation can be realized through a direct digital synthesis (DDS) block (currently based on an AD9953). Tests with an all digital lock-in approach, which samples reference and measurement signal, is also possible, if a fast A/D front-end is added. Currently a head design by our fellow working group is used [10].

The **signal output module** is shown in figure 1.D. It consists of a high precision voltage reference and clock source and three DACs (AD5781, 18Bit, 1Msps) used for fast tip feedback output in Z and X,Y scan signal generation.

A standard PC is used for code development, cross-compilation and data acquisition. Through the use of a network file system (NFS), the control module can exchange code and data transparently with the development system.

When started, the bootloader of the AFM system requests its network configuration over DHCP and downloads the kernel from the development system over TFTP (which permits easy kernel exchange). The root file system is then mounted over NFS. Collected data is either stored on a storage device (SATA hard disk, USB stick) connected to the main module or transmitted over Ethernet to the data acquisition PC.

### 3. Interferometer concept

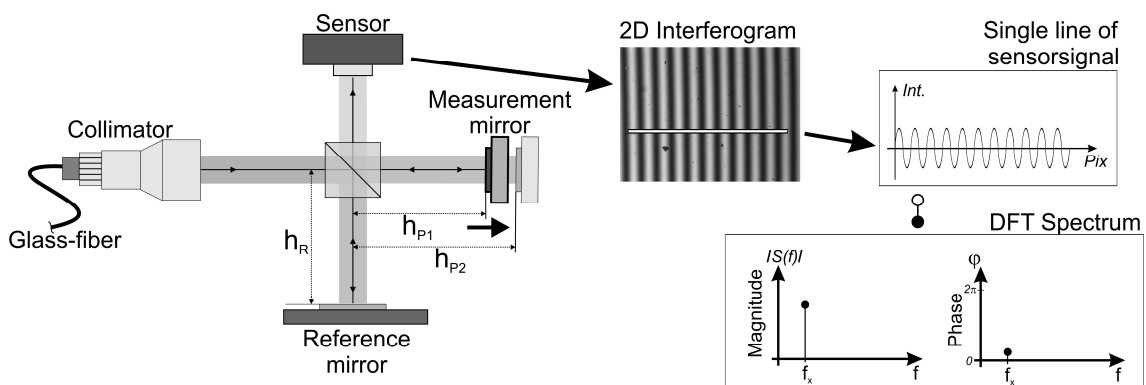


Fig. 2: Conceptual system setup (left). The captured and transformed signal (right).

The interferometer unit resembles a bare-minimum Twyman-Green interferometer (figure 2) consisting of a collimator for light coupling, a 50/50 beam splitter, the reference mirror, the

measurement mirror and an image sensor with an optional objective (not shown). The restriction to a minimum number of optical components reduces errors through multipath reflections and wave front aberrations, saves cost, enables miniaturisation and eases adjustment.

The reference mirror and the measurement mirror are adjusted in a way that a fringe pattern is projected onto the sensor (see figure 2, right). The interferogram consists of a spatial sinusoidal signal whose frequency per unit length depends on the tilt between the reference mirror and the measurement mirror as well as the wavelength of the light source used. The structure of the pattern is directly related to the wavelength of the light source through:

$$\alpha[rad] = \arctan\left(n \cdot \frac{\lambda[nm]}{2 \cdot sensorlength[nm]}\right)$$

With  $\alpha$  the angle between reference and measurement mirror,  $n$  the wavenumber of the main frequency on the sensor and  $sensorlength$  being the length of the applied image sensor.

The captured fringe pattern is converted into the frequency range using the discrete Fourier transform [11] and represented as a magnitude and phase spectrum.

If the measurement mirror is moved, the phase shifts. If the measurement mirror is tilted, the frequency shifts. A separation of multiple superimposed interferograms is possible through different fringe frequencies (correlated with different angles between multiple reference/measurement mirror combinations for multi-axis interferometers) which transform into distinct peaks in the magnitude spectrum. This also allows for an easy separation of nonlinear illumination and dirt (disturbances) from the measurement signal. If the presented system is equipped with a optical reference path, which can be overlaid to the measurement signal, the tracking of unstabilized laser sources is possible and a mode switch or temperature induced drift can be detected and compensated for.

Using the following relation, the movement of the measurement mirror can be calculated from the phase shift in the frequency spectrum, if the initial phase of the spatial pattern is known.

$$\Delta l[nm] = \Delta\varphi[rad] \frac{\lambda[nm]}{2}$$

With  $\Delta l$  displacement,  $\Delta\varphi$  phase difference of the main frequency and  $\lambda$  wavelength of the applied light source. As it is inherent to interferometric systems, the concept is not absolute but periodic with  $2\pi$ , thus a phase unwrapping is necessary. Furthermore an actual implementation of the system needs a repetition rate high enough to follow fast movements without losing track.

#### **4. Interferometer implementation**

While the underlying measurement principle is quite simple, there are some obstacles on the way to a successful implementation.

The optical part of the system has to deal with multiple path reflections, a common phenomenon in interferometric systems. However, in contrast to usual interferometer systems, where these reflections often go unnoticed and the symptom is cured by using the Heydemann correction, due to the nature of the presented system (acquiring spatial images), multiple path reflections are visible to the operator, their origins can be analyzed and they can (hopefully) be eliminated.

In the signal processing part of the system (after capturing the image), one is confronted with a length limited (sensor length) signal, which is quantized in space (pixel) and value (bit depth). The limited signal length works as a rectangular window for the signal. By choice of different window functions (Blackman, von Hann, Kaiser etc.) one can trade of peak width to sidelobe power (which could disturb other nearby additional signals, if a multi signal setup is used), but the Fourier transform of the window function is inevitably present in the spectrum as a convolution with the original signal. For the results shown in this paper, a rectangular window was used. Furthermore in a real application, the captured signal usually does not have an integer number of periods on the sensor. Thus an effect called "leakage" occurs, where signal power is also present in discrete frequency bins adjacent to the main frequency [12]. Sophisticated interpolation schemes can be employed to calculate the actual main frequency, magnitude and phase from its discrete neighbours [11,12,13]. In this work a different approach is tried by using a standard FFT [11], which calculates spectral components at discrete, equidistant frequencies and estimates the signal frequency by interpolation. Subsequently the Goertzel algorithm [11], an infinite impulse response filter to calculate the Fourier transform of a single (non-integer) frequency, is employed to calculate the related magnitude / phase pair.

An additional problem lies in the fact, that the signal is non-negative and unequally illuminated. This offset is transformed as a bump in the low frequency bins of the spectrum; the window function is convoluted with it, thus worsening the problem. To avoid this, the signal has to be conditioned before transformation. In an initialisation step, the signal is analyzed for its amplitude swing at every pixel and an individual offset correction value is calculated, which is applied during the measurement process. The concept could be further extended to an adaptive correction method, but in our tests it remained constant over longer periods of time (>24 hours).

## 5. Measurement results

With the current setup the periodic errors could be reduced below noise level by aforementioned signal processing methods. Figure 3 shows the results for a linear displacement of 2  $\mu\text{m}$ , i.e. approximately six periods (one period equals  $\lambda/2 = 316.5 \text{ nm}$ ).

A PicoCube™ [14] piezo scanner was used in closed-loop mode with its internal capacitive positioning sensors utilized for feedback. The wrapped phase is plotted for reference in Figure 3a. The phase was unwrapped and a linear fit was applied (not shown).

The deviation from this fit, converted to nm, is shown in Figure 3b; it depicts the non-linearity of the piezo stage's internal capacitive sensor. The noise is dominated by the control loop of the piezo scanner and is in the order of 0.1 nm (rms).

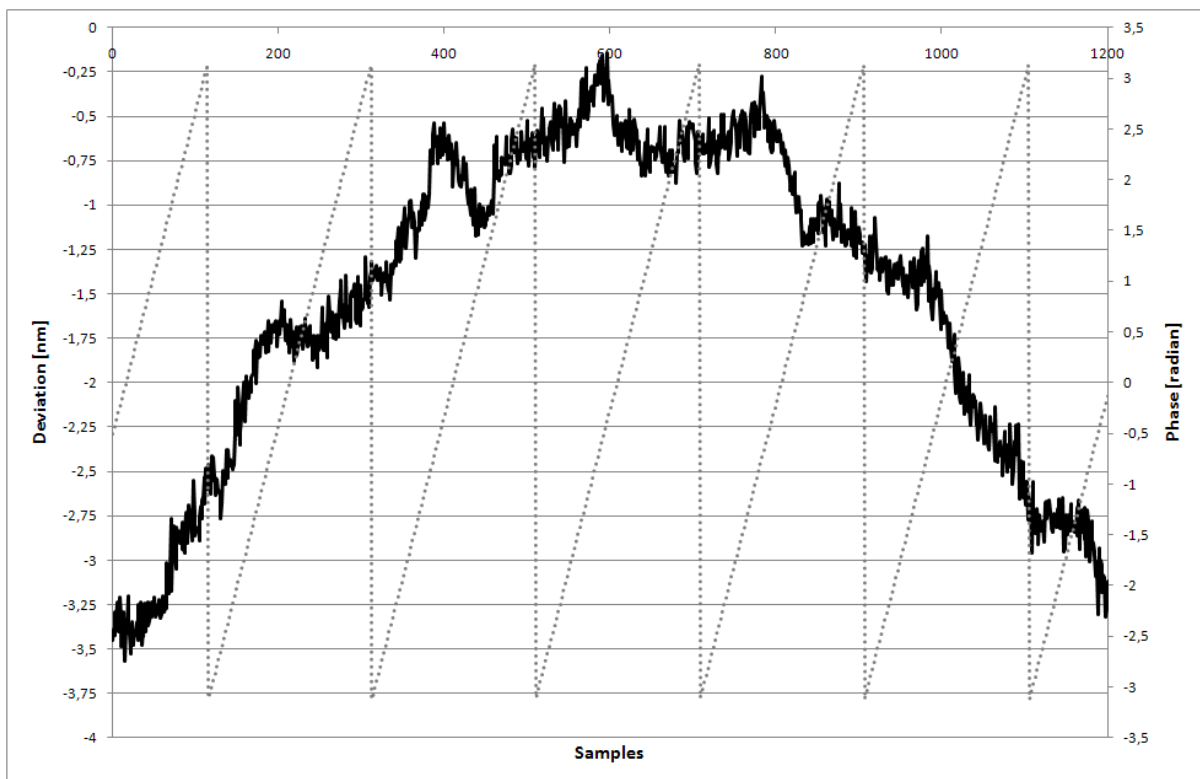


Fig. 3: Measurement results: a) phase (dotted line), b) deviation from linear fit (black)

## 6. Conclusions

A modular, open AFM system, currently in development, is introduced. A new interferometer concept, based on spatial image analysis, to be used in that system is presented. Its realisation as well as problems and their solutions in the optical and signal processing domain are discussed.

## References

- [1] Danzebrink H-U; Koenders L; Wilkening G; Yacoot A, Kunzmann H 2006 Advances in Scanning Force Microscopy for Dimensional Metrology *Annals of the CIRP* 55/2 841 - 879
- [2] Jusko O; Zhao X; Wolff H und Wilkening G 1994 Design and three dimensional calibration of a measuring scanning tunneling microscope for metrological applications. *Rev. Sci. Instrum.* 65, 2514ff
- [3] D. Baigl *et al* 2003 *Europhys. Lett.* **62** doi: 588 10.1209/epl/i2003-00391-2
- [4] Dai G, Pohlenz F; Danzebrink H-U; Xu M; Hasche K; Wilkening G 2004 Metrological large range scanning probe microscope *Rev. Sci. Instrum.* 75 4, 962-969
- [5] Jäger G, Manske E, Hausotte T, Büchner H-J, Grünwald R and Schott W 2001, Nanometrology - nanomeasuring machines *Proc. Annual meeting of ASPE, Crystal City, Virginia, USA, 23-27.*
- [6] Gonda, S., Doi, T., Kurosawa, T., Tanimura, Y., Hisata, N., Yamagishi, T., Fujimoto, H., Yukawa, H., 1999, Real-time, interferometrically measuring atomic force microscope for direct calibration of standards, *Rev. Sci. Instr.*, 70:3362-3368.
- [7] Picotto, G.B., M. Pisani, M., 2001, A sample scanning system with nanometric accuracy for quantitative SPM measurements, *Ultramicroscopy*, 86:247-254.
- [8] Texas Instruments, OMAP-L138 C6-Integra™ DSP+ARM® Processor,  
<http://focus.ti.com/lit/ds/symlink/omap-l138.pdf>
- [9] e2v, EV76C560 B&W and Colour CMOS Sensor,  
[http://www.e2v.com/assets/media/files/brochures-flyers/25-05%20E2V%20Fiche%20CMOS\\_B%20EV76C560.pdf](http://www.e2v.com/assets/media/files/brochures-flyers/25-05%20E2V%20Fiche%20CMOS_B%20EV76C560.pdf)
- [10] Hwu E-T, Illers H, Jusko L and Danzebrink H-U 2009 A hybrid scanning probe microscope (SPM) module based on a DVD optical head. *Meas. Sci. Technol.* 20 084005 (8pp); doi: 10.1088/0957
- [11] Oppenheim A V, Schafer R W Discrete-time signal processing 2<sup>nd</sup> .ed. *Prentice Hall Internatinal, Inc. ISBN 0-13-083443-2*
- [12] Lyons R G, Understanding digital signal processing 2<sup>nd</sup> ed. *Pearson Education, Inc. ISBN 0-13-108989-7*
- [13] Meyer-Baese U, Digital Signal Processing with Field Programmable Gate Arrays 3<sup>rd</sup> ed. *Springer Verlag, ISBN 978-3-540-72612-8*
- [14] Physik Instrumente, P-363 PicoCube™ XY/XYZ Piezo Scanner,  
<http://www.physikinstrumente.com/en/products/prdetail.php?sortnr=201650>